WILEY-VCH

DOI: 10.1002/((please add manuscript number))
Article type: Communication

Self-assembly of functionalized oligothiophene into hygroscopic fibers: fabrication of highly sensitive and fast humidity sensors

*Marco A. Squillaci,[1] Alessio Cipriani,[1,2] Manuela Melucci,[3] Massimo Zambianchi,[3] Grabriella Caminati[2] and Paolo Samorì[1]**

Dr. M. A. Squillaci, A. Cipriani, Prof. P. Samorì
University of Strasbourg CNRS, ISIS UMR 7006, 8 allée Gaspard Monge, F-67000 Strasbourg, France.
E-mail: samori@unistra.fr

Dr. E. Melucci, M. Zambianchi
CNR-ISOF, Via P. Gobetti 101, 40129 Bologna, Italy.

A. Cipriani, Prof. G. Caminati
Dipartimento di Chimica "Ugo Schiff", Via della Lastruccia 3-13, 50019
Sesto Fiorentino, Italy.

Keywords: humidity sensors, supramolecular fibers, bolaamphiphilic molecules, self-assembly, oligothiophenes

Abstract

A new symmetric oligothiophene exposing tetraethylene glycol (TEG)-based side-chains has been designed and synthesized. This molecule was found to self-assemble in solution forming supramolecular fibers, via π-π stacking between the conjugated oligothiophene backbones, which are phase segregated on the sub-nm scale from the TEG side-groups. The delocalization of the charges through the oligothiophene π-π stack ensures efficient charge transport while the hygroscopic shell decorating the surface of the fibrillar structures determines a certain affinity for polar molecules. Upon exposure to humidity, under environmental conditions, such supramolecular architectures are capable of reversibly absorb and desorb water molecules. Absorption of water molecules due to increased environmental humidity, causes a fast and reproducible increase of the current through the fibers by a factor 100 from 15% to 90% relative humidity as measured in 2-terminal devices. Such process is extremely fast, taking place in less than 45 ms. The humidity-responsive characteristics of the presented oligothiophene-based fibers can be exploited for the facile fabrication of high-performances and solution-processable electrical resistive humidity sensors.

Control of the environmental humidity is of paramount importance not only for numerous industrial and technological processes but also to guarantee the comfort of live beings, improving the quality of life in living and working places.[1] Because of this reason, during the last years a great effort has been devoted to the development of humidity sensing devices featuring high-speed, low-power consumptions and smaller sizes.[2] Hitherto, different geometries and sensing mechanisms have been explored to improve one or more of such aspects, involving the use of direct electrical readouts (such as changes in devices's resistance,[3] capacitance[4] or gate effect in field-effect transistors[5]) as well as indirect ones (such as optical[6, 7] readouts or small mass changes[8]). In a humidity sensors, the active material has the role of interacting with water molecules, quantitatively translating such interaction into a readable output. So far different active materials have been explored, including ceramics,[1, 9] metal nanoparticles,[10] carbon-based materials,[11] composites[12] and organic/polymeric thin films.[6]

Since the absorption and recognition processes takes place on the surface of the active material, a viable strategy in order to harness higher performances relies on the use of low-dimensional nanostructures, fully decorated with *ad-hoc* receptors of the analyte of interest. In this framework, molecular self-assembly offers unparalleled versatility to design and control the formation of functional low-dimensional structures, featuring intermolecular order up to the micrometer scale.[13] Self-assembled aggregates of conjugated molecules have shown to be promising candidates as active materials for numerous applications, including photovoltaics,[14] field-effect transistors[15] and photo-resists.[16] In humidity sensing, supramolecularly engineered one-dimensional architectures have been successfully employed to achieve state-of-the-art performance in terms of sensitivity[17] and response speed.[18] Supramolecular chemistry also offers a broadest arsenal of highly selective receptors of any analyte of interest. For the specific

case of H_2O molecules, ethylene glycol oligomers and polymers have shown to be ideal scaffolds, exhibiting hygroscopicity and undergoing reversible structural changes upon interaction with moisture.[19]

Here we report on a newly synthesized molecular scaffold, consisting of a π-conjugated oligomeric backbone bearing hydrophilic chains as end substituents. Specifically, the chosen oligomer consists of a conjugated oligothiophene (OT) backbone capped with phenyl groups bearing tetraethylene glycol (TEG) side chains which are attached in the α and ω positions of the backbone (**Figure 1 and S1**). Under certain strict conditions of solvent and temperature, this molecule spontaneously undergoes self-assembly forming supramolecular fibers (**Figure 1**), characterized by π-π stacking between the OT backbones, and exposing hydrophilic TEG chains in the external sheath. Such fibers exhibit humidity-dependent electrical characteristics, thus they can function as active materials for the fabrication of high-performances solution-processed electrical resistive humidity sensors.

The target OT-TEG compound (**6**), was prepared in high yield (90%) starting from 5-bromo-1,2,3-tris(2-(2-(2-methoxyethoxy)ethoxy)ethoxy) benzene (**1**),[20] through a synthetic sequence consisting of sequential Suzuki-Miyaura coupling to compound **3**, bromination and final Still coupling reaction with bistannylbithiophene derivative **5** (Figure S1).

The structure of our molecule, exhibiting a hydrophobic core and two symmetric hydrophilic side chains, induces a bolaamphiphilic behavior of the system and the tendency to self-assemble into supramolecular architectures exhibiting a high aspect ratio.[21] The simultaneous presence of hydrophobic and hydrophilic groups makes this molecule soluble in polar solvents, such as water, as well as in non-polar ones, such as chloroform and cyclohexane. Depending on the polarity of the solvent, these molecules interact differently among each other, resulting in a

strong solvatochromic effect, given by the intermolecular aggregation between the cores, which affects both the UV-Vis absorbance and the fluorescence emission spectra in solution, as visible in **Figure S2**. As reported in literature for similar systems, the use of polar solvents should trigger the face-to-face self-assembly of the oligothiphene cores into J-aggregates.[22] With the aim of finding the best experimental conditions to grow conductive OT-TEG supramolecular fibers, in which all the aromatic cores form J-aggregates via π-π stacking, we have performed a systematic study by exploring different solvents and concentrations. The special optical properties of these molecular building block in solution were studied and exploited in order to gain insight into the aggregation at the molecular level. Such studies revealed that the best compromise between solubility and solvent-induced aggregation is obtained in methanol solutions at a concentration $C \sim 4 \cdot 10^{-5}$ M. Under these conditions the aggregation of the OT-TEG molecules can be triggered by lowering the temperature, resulting in a strong thermochromic behavior which affects both the UV-Vis absorbance and the emission characteristics, as highlighted in **Figure S3 and S5**. In particular, by lowering the temperature from 55° C to 5° C, the main UV-Vis absorbance band at $\lambda = 446$ nm is gradually red shifted, up to $\lambda = 465$ nm, and a new shoulder at $\lambda = 535$ nm appears. The effect of temperature on the fluorescence spectra is even more pronounced than the one observed in the UV-Vis absorbance measurements: by lowering the temperature within the same range, the main peak at $\lambda = 532$ nm undergoes a strong quenching; the peak originally located at $\lambda = 561$ nm undergoes quenching and red-shift and, finally a third peak, located at $\lambda = 634$ nm, appears at $T \leq 15$° C. As reported in **Figure S6**, such modifications of the optical features of OT-TEG methanol solutions are reversible and are indicative of the formation of intermolecular J-aggregates involving π-π stacking between the conjugated cores of OT-TEG which cause an intermolecular delocalization

of the π electrons and a subsequent decrease of the molecular bandgap.[23] Such aggregation causes a red-shift of the UV-Vis absorbance and a contemporary quenching of the photoluminescence characteristics of the system. As visible in **Figure S4**, the melting temperatures of the OT-TEG supramolecular aggregates in such methanol solution is~18° C. The deposition of the latter solutions on solid supports was performed by drop-casting onto the basal plane of hydrophobic Si/SiO_2, functionalized with a chemisorbed self-assembled monolayer of hexamethyldisilazane (HMDS) which is used to increase hydrophobicity thereby promoting the growth of larger columnar aggregates via π-π stacking interactions.[23] Such process leads to the formation of fibrillar structures featuring lengths of several tens on micrometers and variable widths, as shown in the fluorescence microscopy and in the SEM images in **Figure 2a,b**. To gain a deeper insight into the morphology of such aggregates, atomic force microscopy (AFM) topography images were recorded. AFM characterization revealed that the fibrillar structures observed by optical microscopy consist of bundles of smaller fibers, exhibiting an average width of 60 ± 10 nm, as visible in **Figure 2c and S7**. The 3D AFM topographic map portrayed in **Figure 2d** allows to highlight the bundled nature of such structures and reveals the presence of nodes in which multiple fibers are overlapped., Such observation suggests that formation of the supramolecular fibers takes place in solution rather than on the substrate whereas the generation of superstructures made of multiple intertwined fibers occurs as a result of the drying-up process when the solution is drop-cast on the surface. Such a two-steps self-assembly process is in agreement with the discussion above on the optical properties of OT-TEG in solution.

As aforementioned, aggregation of OT-TEG in polar solvents, such as methanol, should lead to the formation of fibrillary structures made by J-aggregates in which the conjugated thiophene

cores interact between each other via π-π stacking, as schematized in Figure 1. According to this model the resulting OT-TEG fibers should exhibit electrical (semi)conducting behavior.

In order to test their electrical characteristics, the OT-TEG supramolecular fibers were deposited by using the same approach discussed above, on Si/SiO_2 substrates pre-patterned with gold interdigitated electrodes featuring channel lengths ranging from 2.5 μm to 20 μm. As shown in the AFM and optical microscopy images in **Figure S8 and S9**, the resulting supramolecular fibers are randomly dispersed over the contact area, bridging the electrodes. Two-terminal electrical characterization of such aggregates in low humidity environments revealed a high electrical resistance of 8.0 ± 0.3 GΩ which is almost independent from the employed channel length, as displayed in **Figure S10**.

Moreover, by performing multiple I-V scan cycles under the same conditions, it is possible to observe a gradual decrease of the current flowing through the devices. Such phenomena is reversible with time and can be attributed to a bias stress given by the high resistivity of the system in low humidity environments (**Figure S12**).

The presence of TEG groups as an external shell decorating the whole surface of the fibers, enables enhanced sensitivity and responsivity to moisture. In particular, water molecules from the atmosphere can be absorbed and reversibly trapped/released within the hygroscopic TEG branches on the fiber's surface. Absorbed water molecules behave as a bridge between intermolecular TEG chains, using H-bonding to disrupt the electrostatic repulsion, ultimately improving the packing within the fibers and decreasing the intermolecular π-π distance. Such subtle structural modifications have a dramatic impact on the transfer integral and therefore on the electrical current passing through the fibers via intermolecular hopping.[17, 24]

In order to test the capability of OT-TEG fibers to interact with water vapor and to verify the aforementioned interaction model, the electrical characteristics of our devices were exploited as an extremely sensitive probe to follow such sub-nanometer changes in the intermolecular packing of the building blocks. Such measurements were performed in two different ways to assess information over (i) speed and reversibility of the water absorption, and (ii) to estimate the stability over time and the maximum humidity-induced current shift. The first kind of measurements were carried out by sending short pulses of humid air directly onto the sample's surface while applying a constant drain bias of 1 V and continuously measuring the drain current (**Figure 3a** and **Figure S14**). The calibrations to quantitatively correlate the changes in drain current with the environmental humidity, were performed by placing the sample in a sealed environment with controlled relative humidity (RH) within the range from 15% to 90% (**Figure 3b**). The plot in Figure 3a displays the typical quick response of our OT-TEG devices to short pulses of humid air. Such measurements show that the water absorption process is fully reversible and extremely fast, with absorption and response time < 45 ms and recovery time of 300 ms. By performing several hundred of fast cycles like the ones reported in figure 3a the sensors did not show any sign of degradation nor drop of performances. However, a precise evaluation of the response time cannot be provided, because, as displayed in the inset of Figure 3a, the sampling time of the source meter employed for such characterization is limited to 45 ms, due to the high resistivity of the devices. From the calibration plot depicted in Figure 3b it is possible to observe that the measured drain current changes exponentially with the relative humidity causing an overall current shift as big as two orders of magnitude (a factor of 100) between dry (RH = 15%) and humid (RH = 90%) environments. Interestingly, a comparison of the responses from different devices featuring different channel lengths (2.5 μm and 5 μm)

revealed that the devices with shorter channel length exhibit slightly higher sensitivity, probably due to the lower bias stress affecting shorter channels (more details and non-normalized calibration plot can be found in **Figure S13**).

In summary, we have synthesized a new molecular building block featuring a bolaamphiphilic structure made by a hydrophobic oligothiophene conjugated core and symmetric tetraethylene glycol-based hydrophilic side chains. Such molecular building block can be self-assembled in methanol solution into supramolecular fibers. Drop-casting of such solutions on hydrophobic substrates results in the formation of one-dimensional fibrillar architectures with a bundled and entangled structure. Electrical characterizations have shown that the presence of the symmetric and sterically hindered side chains, causes a long distance packing between the oligothiophene cores within the aggregates, resulting in an extremely high electrical resistance in low humidity conditions. Exposure of such supramolecular fibers to moisture allows water molecules to bridge the side chains, aligning the building block and reducing the π-π stacking distance among adjacent molecules.[18, 24] The reduced π-π stacking distance causes an exponential increase of the electrical current flowing through the fibers which is proportional to the relative humidity in the atmosphere surrounding the devices. This characteristic has been exploited for the fabrication of high performance electrical resistive humidity sensors which can be solution-processed with a facile and straightforward approach. The fabricated sensors have shown high sensitivity, featuring a uniform and predictable current shift as large as two orders of magnitude from 15% and 90% relative humidity, which is also fully reversible. Moreover such devices feature stability over an undefined amount of cycles, recovery time of 300 ms and a remarkable response time of < 45 ms which is in line with graphene oxide-based sensors (response time ~ 30 ms)[11] and with the state-of-the-art supramolecular devices which feature response time of ~ 10 ms.[18]

Experimental Section

Experimental details can be found in the Supporting Information.

Supporting Information

Supporting Information is available from the Wiley Online Library or from the author.

Acknowledgements

This work was financially supported by EC through the ERC project SUPRAFUNCTION (GA-257305) and the Marie Sklodowska-Curie ITN projects iSwitch (GA No. 642196) and SYNCHRONICS (GA No. 643238), the ANR Labex project CSC (ANR-10- LABX-0026 CSC) within the Investissement d'Avenir program ANR-10-IDEX-0002-02, and the International Center for Frontier Research in Chemistry (icFRC).

Received: ((will be filled in by the editorial staff))
Revised: ((will be filled in by the editorial staff))
Published online: ((will be filled in by the editorial staff))

References

[1] E. Traversa, *Sensor Actuat B-Chem* **1995**, *23*, 135.
[2] H. Farahani, R. Wagiran, M. N. Hamidon, *Sensors* **2014**, *14*, 7881; A. Oprea, J. Courbat, N. Barsan, D. Briand, N. F. de Rooij, U. Weimar, *Sensor Actuat B-Chem* **2009**, *140*, 227.
[3] X.-M. Jiang, Z.-B. Yan, D. Liu, K.-F. Wang, G.-C. Guo, S.-Z. Li, J.-M. Liu, *Chem Asian J* **2014**, *9*, 2872.
[4] H. P. Hong, K. H. Jung, J. H. Kim, K. H. Kwon, C. J. Lee, K. N. Yun, N. K. Min, *Nanotechnology* **2013**, *24*, 085501.
[5] F. Liang, L.-B. Luo, C.-K. Tsang, L. Zheng, H. Cheng, Y. Y. Li, *Mater Res Bull* **2012**, *47*, 54.
[6] E. Kim, S. Y. Kim, G. Jo, S. Kim, M. J. Park, *ACS Appl Mater Interfaces* **2012**, *4*, 5179.
[7] W. C. Wong, C. C. Chan, L. H. Chen, T. Li, K. X. Lee, K. C. Leong, *Sensor Actuat B-Chem* **2012**, *174*, 563.
[8] J. Xie, H. Wang, Y. Lin, Y. Zhou, Y. Wu, *Sensor Actuat B-Chem* **2013**, *177*, 1083.
[9] (a) C. Doroftei, P. D. Popa, F. Lacomi, *Sensor Actuat a-Phys* **2012**, *173*, 24; (b) R. K. Kotnala, J. Shah, B. Singh, H. Kishan, S. Singh, S. K. Dhawan, A. Sengupta, *Sensor Actuat B-Chem* **2008**, *129*, 909; (c) V. Jeseentharani, L. Reginamary, B. Jeyaraj, A. Dayalan, K. S. Nagaraja, *J Mater Sci* **2012**, *47*, 3529.
[10] H. C. Lee, C. Y. Wang, C. H. Lin, *Sensor Actuat B-Chem* **2014**, *191*, 204.

[11] S. Borini, R. White, D. Wei, M. Astley, S. Haque, E. Spigone, N. Harris, J. Kivioja, T. Ryhanen, *ACS Nano* **2013**, *7*, 11166.
[12] (a) Y. Zilberman, R. Ionescu, X. Feng, K. Mullen, H. Haick, *ACS Nano* **2011**, *5*, 6743; (b) W. D. Lin, H. M. Chang, R. J. Wu, *Sensor Actuat B-Chem* **2013**, *181*, 326; (c) S. Pokhrel, B. Jeyaraj, K. S. Nagaraja, *Mater Lett* **2003**, *57*, 3543.
[13] (a) I. McCulloch, M. Heeney, C. Bailey, K. Genevicius, I. Macdonald, M. Shkunov, D. Sparrowe, S. Tierney, R. Wagner, W. M. Zhang, M. L. Chabinyc, R. J. Kline, M. D. McGehee, M. F. Toney, *Nat Mater* **2006**, *5*, 328; (b) J. M. Mativetsky, M. Kastler, R. C. Savage, D. Gentilini, M. Palma, W. Pisula, K. Mullen, P. Samori, *Adv Funct Mater* **2009**, *19*, 2486; (c) R. van Hameren, P. Schon, A. M. van Buul, J. Hoogboom, S. V. Lazarenko, J. W. Gerritsen, H. Engelkamp, P. C. M. Christianen, H. A. Heus, J. C. Maan, T. Rasing, S. Speller, A. E. Rowan, J. Elemans, R. J. M. Nolte, *Science* **2006**, *314*, 1433; (d) T. Aida, E. W. Meijer, S. I. Stupp, *Science* **2012**, *335*, 813; (e) W. Zhang, W. Jin, T. Fukushima, A. Saeki, S. Seki, T. Aida, *Science* **2011**, *334*, 340; (f) T. Sakurai, K. Tashiro, Y. Honsho, A. Saeki, S. Seki, A. Osuka, A. Muranaka, M. Uchiyama, J. Kim, S. Ha, K. Kato, M. Takata, T. Aida, *J Am Chem Soc* **2011**, *133*, 6537.
[14] (a) Y. Kim, S. Cook, S. M. Tuladhar, S. A. Choulis, J. Nelson, J. R. Durrant, D. D. C. Bradley, M. Giles, I. McCulloch, C. S. Ha, M. Ree, *Nat Mater* **2006**, *5*, 197; (b) F. Fuchs, M. Linares, C. de Vet, P. Leclere, R. Demadrille, B. Grevin, *Adv Mater* **2014**, *26*, 6416; (c) T. Ye, R. Singh, H. J. Butt, G. Floudas, P. E. Keivanidis, *ACS Appl Mater Interfaces* **2013**, *5*, 11844.
[15] (a) J. M. Mativetsky, E. Orgiu, I. Lieberwirth, W. Pisula, P. Samori, *Adv Mater* **2014**, *26*, 430; (b) C. B. Nielsen, M. Turbiez, I. McCulloch, *Adv Mater* **2013**, *25*, 1859; (c) R. Pfattner, E. Pavlica, M. Jaggi, S.-X. Liu, S. Decurtins, G. Bratina, J. Veciana, M. Mas-Torrent, C. Rovira, *J. Mater. Chem. C* **2013**, *1*, 3985.
[16] M. A. Squillaci, F. Qiu, A. Aliprandi, F. Zhang, X. L. Feng, P. Samori, *Adv. Mater.* **2016**, *28*, 5249.
[17] M. A. Squillaci, L. Ferlauto, Y. Zagranyarski, S. Milita, K. Mullen, P. Samori, *Adv. Mater.* **2015**, *27*, 3170.
[18] U. Mogera, A. A. Sagade, S. J. George, G. U. Kulkarni, *Sci Rep* **2014**, *4*, 4103.
[19] (a) B. Bilen, Y. Skarlatos, G. Aktas, M. N. Inci, T. Dispinar, M. M. Kose, A. Sanyal, *J. Appl. Phys.* **2007**, *102*, 6; (b) H. M. L. Thijs, C. R. Becer, C. Guerrero-Sanchez, D. Fournier, R. Hoogenboom, U. S. Schubert, *J Mater Chem* **2007**, *17*, 4864.
[20] C. Nagamani, J. Guo, S. Thayumanavan, *J. Polym. Sci., Part A: Polym. Chem.* **2012**, *50*, 1187.
[21] B. Song, G. Liu, R. Xu, S. Yin, Z. Wang, X. Zhang, *Langmuir* **2008**, *24*, 3734.
[22] (a) A. F. M. Kilbinger, W. J. Feast, *J Mater Chem* **2000**, *10*, 1777; (b) D. Fichou, *J Mater Chem* **2000**, *10*, 571.
[23] P. Leclère, M. Surin, P. Viville, R. Lazzaroni, A. F. M. Kilbinger, O. Henze, W. J. Feast, M. Cavallini, F. Biscarini, A. P. H. J. Schenning, E. W. Meijer, *Chem Mater* **2004**, *16*, 4452.
[24] A. Bhattacharyya, M. K. Sanyal, U. Mogera, S. J. George, M. K. Mukhopadhyay, S. Maiti, G. U. Kulkarni, *Sci. Rep.* **2017**, *7*, 246.

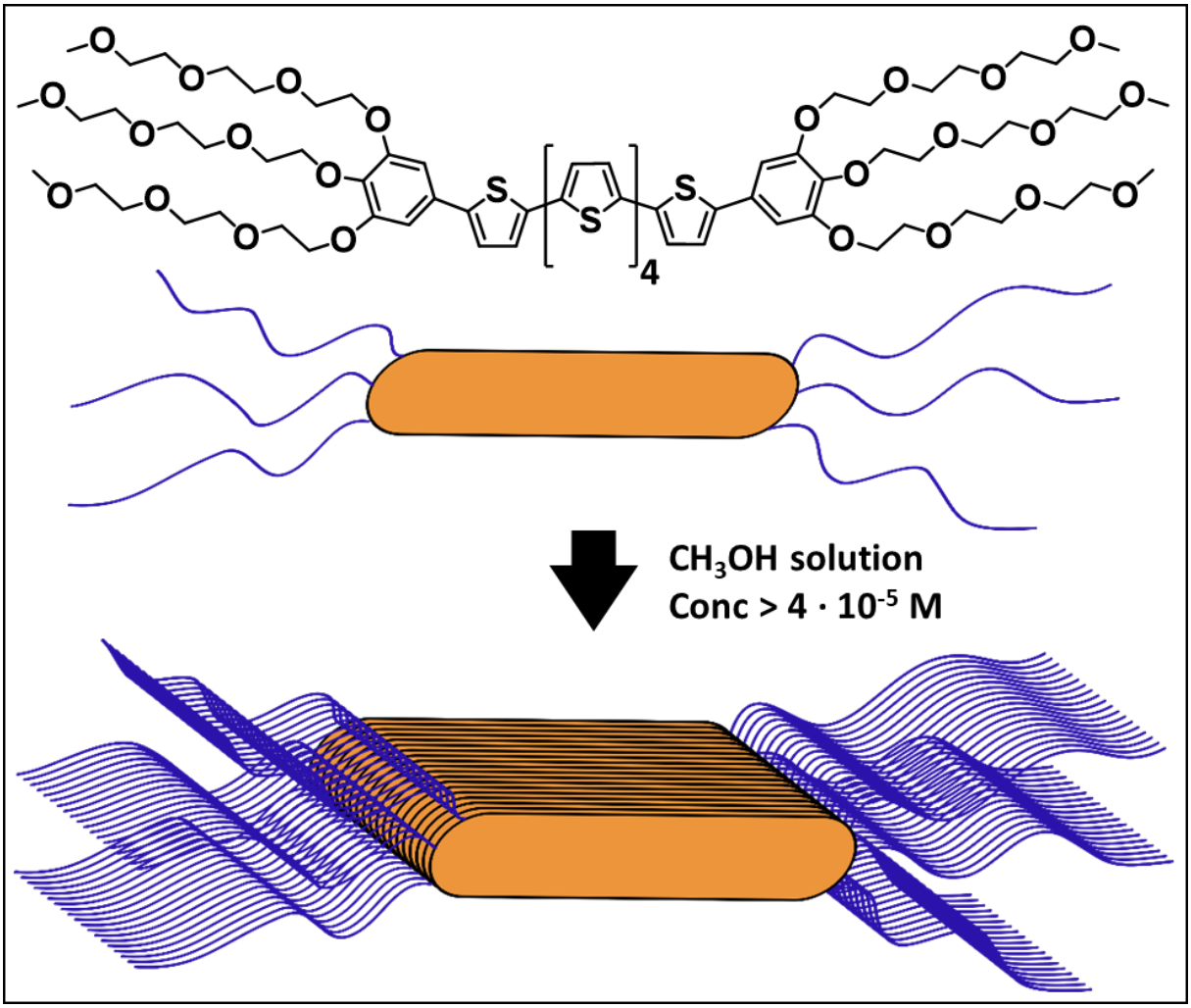

Figure 1: Molecular structure of OT-TEG and proposed self-assembly into 1-dimensional structures in methanol solution.

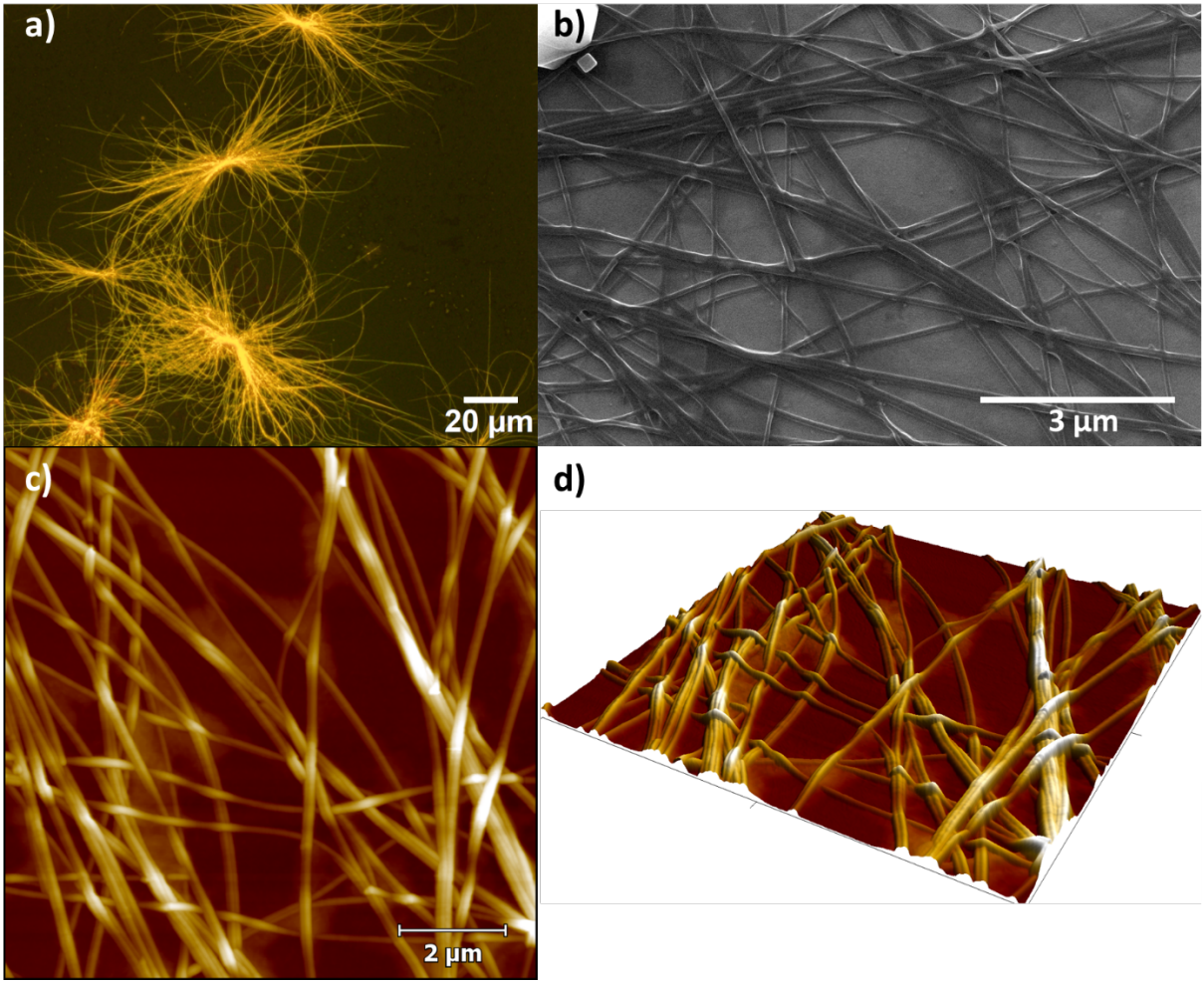

Figure 2: Fibrillar supramolecular structures of OT-TEG drop-cast on hydrophobic Si/SiO_2. a) Fluorescence microscopy image showing seeded growth of the aggregates. b) SEM image. c) AFM topography images displaying entangled bundles of fibers. d) 3D rendering of the AFM image highlighting the bundled nature and the entanglement between the OT-TEG fibers. (AFM images Z scale = 360 nm)

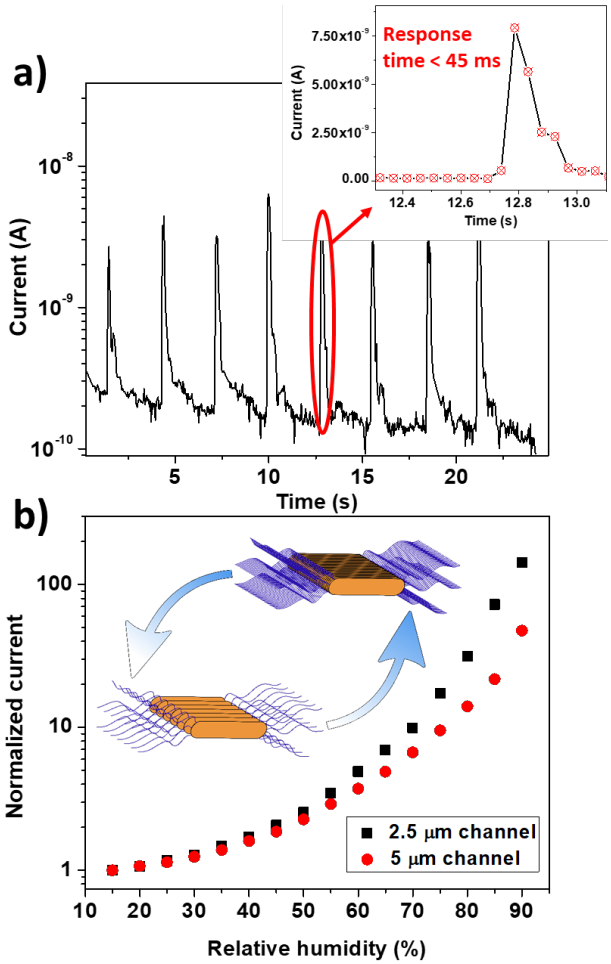

Figure 3: Electrical resistive humidity sensing characteristics of OT-TEG fibers. a) Measurements of response speed and reversibility of the water absorption (Constant drain bias applied = 1 V). b) Normalized calibration curves for interdigitated devices with 2.5 µm and 5 µm channel lengths.